

Adsorption-Desorption Kinetics of Soft Particles

Brendan Osberg, Johannes Nuebler, and Ulrich Gerland*

*Theory of Complex Biosystems, Physik-Department, Technische Universität München,
James-Frank-Strasse 1, 85748 Garching, Germany*

(Received 27 April 2015; published 18 August 2015)

Adsorption-desorption processes are ubiquitous in physics, chemistry, and biology. Models usually assume hard particles, but within the realm of soft matter physics the adsorbing particles are compressible. A minimal 1D model reveals that softness fundamentally changes the kinetics: Below the desorption time scale, a logarithmic increase of the particle density replaces the usual Rényi jamming plateau, and the subsequent relaxation to equilibrium can be nonmonotonic and much faster than for hard particles. These effects will impact the kinetics of self-assembly and reaction-diffusion processes.

DOI: 10.1103/PhysRevLett.115.088301

PACS numbers: 82.70.Dd, 87.10.Mn, 87.15.R-

A broad range of physical, chemical, and biological systems feature adsorption processes in which particles are randomly deposited on an extended substrate [1]. Possible substrates include polymers [2], crystalline or amorphous surfaces [3], and membranes, while the particles can be small molecules, colloidal particles, macromolecules such as proteins [4,5], or even larger objects such as cells. In phenomenological models [6–8], the particles can also represent modified states of the substrate [6] or complexes formed with the substrate [8]. Generally, the filling of the substrate slows as the coverage increases, due to substrate saturation as well as jamming. Here, jamming refers to the process of reaching configurations where all gaps are smaller than the particles, prohibiting further filling. Jammed configurations constitute a nonthermal ensemble that has received considerable theoretical interest [9,10]. However, jamming is often only transient, as a small desorption rate allows the system to eventually reach thermal equilibrium in a nontrivial relaxation process during which the system loses memory of its jammed state [11–13].

Adsorption-desorption models usually assume hard particles that can neither be deformed nor overlap on the substrate. This assumption does not hold for systems such as soft colloidal particles [14], macromolecules like proteins [5], or complexes that can be forced into conformations with different effective sizes [15]. While the mechanical properties of soft particle systems are well studied [16], their adsorption-desorption kinetics have not been characterized. To explore this question, we analyze a minimal model with particles of finite stiffness ϵ binding to a one-dimensional (1D) substrate; see Fig. 1. Our model recovers the hard particle kinetics in the $\epsilon \rightarrow \infty$ limit but demonstrates that the new parameter significantly enriches the kinetic behavior. Notably, softness can lead to nonmonotonic filling, where an initially empty substrate fills to a high “cramming density” ρ_{cr} before relaxing to the equilibrium density $\rho_{\text{eq}} < \rho_{\text{cr}}$. While this behavior may

seem counterintuitive, it does not violate thermodynamic principles.

Our model is a generalization of the 1D car parking model [11,12] to soft particles. Models of this type are directly applicable to experimental systems with linear topology, and they also serve as a tractable theoretical framework to capture general kinetic phenomena [1]. For instance, 1D models show how the extremely slow relaxation of jammed systems [11,12] arises from the growing number of rearrangements required to make space for additional particles [13]. The same physics applies also in higher dimensions, e.g., to describe the slow densification of vibrated granular materials [13,17–19]. We discuss general implications of our 1D results further below.

Model.—Our model, illustrated in Fig. 1, describes the random adsorption and desorption of soft particles on a 1D substrate. The particles are assumed to have a finite interaction range set to 1, defining the length unit. Isolated particles adsorb at the bare rate r_+ per unit length and desorb with rate r_- . We are interested in the regime in which the rate ratio

$$r = r_+/r_- = e^\mu \quad (1)$$

is large, such that adsorption and desorption operate on very different time scales and a high equilibrium density is

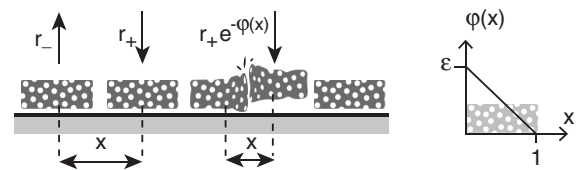


FIG. 1. One-dimensional adsorption-desorption model for soft particles. Overlapping adsorptions that require deformation are allowed but slowed down by the Boltzmann factor of the interaction energy $\phi(x)$, which depends linearly on the center-to-center distance x . In the limit $\epsilon \rightarrow \infty$ the hard particle model is recovered.

ultimately reached. For later convenience, Eq. (1) expresses r also in terms of the chemical potential of the non-interacting system, μ (throughout this Letter we set $k_B T = 1$ by choice of energy unit). A soft particle can attach even if it partially overlaps with its neighbor(s). We assume that overlaps are associated with an interaction $\varphi(x)$, where x denotes the center-to-center distance of adjacent particles. We primarily consider a potential that increases in proportion to proximity,

$$\varphi(x) = \begin{cases} \varepsilon(1-x) & \text{for } x \leq 1, \\ 0 & \text{for } x > 1, \end{cases} \quad (2)$$

but also test to what extent the kinetic behavior depends on the shape of $\varphi(x)$. We note that potentials with finite stiffness ε can also serve as effective descriptions for hard particles that fluctuate between internal states with different effective lengths.

The interaction (2) modulates the reaction rates. An adsorption event alters the total interaction energy by $U(x_L, x_R) = \varphi(x_L) + \varphi(x_R) - \varphi(x_L + x_R)$, with the center-to-center distances to the left and right neighbors, x_L and x_R . Detailed balance requires that the modulated rates \tilde{r}_+ , \tilde{r}_- have the ratio $e^{\mu-U}$. As we do not seek to describe a specific experimental system, but rather to characterize generic effects of softness on adsorption-desorption kinetics, we can simply choose $\tilde{r}_- = r_-$ and

$$\tilde{r}_+(x_L, x_R) = r_+ e^{-U(x_L, x_R)}. \quad (3)$$

The Supplemental Material [20] discusses the effects of distributing the Boltzmann factor between adsorption and desorption.

Our model does not explicitly include lateral diffusion, although an effective form of lateral transport arises via desorption and readsorption [22]. We analyze the full stochastic kinetics of our model with simulations using the Gillespie method [23]. We also use a mean field description that characterizes the state of the system by the line density of particle spacings, $V(x, t)$, which obeys

$$\begin{aligned} \frac{\partial}{\partial t} V(x, t) = & 2 \int_x^\infty dy V(y, t) \tilde{r}_+(x, y-x) - 2r_- V(x, t) \\ & - V(x, t) \int_0^x dy \tilde{r}_+(y, x-y) \\ & + r_- \int_0^x dy \frac{V(y, t)V(x-y, t)}{\rho(t)} \end{aligned} \quad (4)$$

and $\int_0^\infty dx x V(x, t) = 1$ (conservation of space). Since the number of voids equals the number of particles, the total particle density is $\rho(t) = \int_0^\infty dx V(x, t)$. Equation (4) describes the creation and destruction of voids of size x via adsorption within larger voids, desorption of a bounding particle, adsorption within the void, and the fusion of

two smaller voids. In the last term of Eq. (4) the two-void density is approximated by the product of one-void densities, truncating the hierarchy of mean field equations at lowest order. Equation (4) recovers the mean field description of the car parking model [12] in the limit $\varepsilon \rightarrow \infty$. For $t \rightarrow \infty$, the equilibrium distribution $V_{\text{eq}}(x) \propto e^{-\alpha x - \varphi(x)}$ is reached [20]. The equilibrium density can exceed unity since particles can overlap. See Ref. [20] for a comparison of the mean field and full model, the lattice equivalent of Eq. (4) used for all simulations, and a discussion of finite size effects.

Qualitative behavior.—Figure 2 characterizes the filling kinetics of an initially empty substrate. The time evolution of the total particle density $\rho(t)$ is shown in Fig. 2(a) for different stiffnesses ε , including the hard-core limit $\varepsilon \rightarrow \infty$. On the logarithmic time axis, the two time scales $1/r_+$ and $1/r_-$ roughly divide the kinetics into three separate stages. (i) Essentially unhindered adsorption for $t < 1/r_+$ with $\rho(t) \sim t$ independent of ε since interactions play only a minor role initially. At the end of this stage, most voids large enough for nonoverlapping adsorption are exhausted. (ii) For $1/r_+ < t < 1/r_-$, hard-core particles are in a jamming stage: Their density remains essentially constant at a plateau of $\rho_{\text{jam}} \approx 0.748$, the Rényi limit [9]. In contrast, the density of soft particles keeps increasing, albeit only logarithmically, $\rho(t) - \rho_{\text{jam}} \sim \log(t)$. (iii) In the third stage, $t > 1/r_-$, desorption becomes relevant and all systems relax to their equilibrium density ρ_{eq} . However, the relaxation behavior changes dramatically with ε . Whereas the

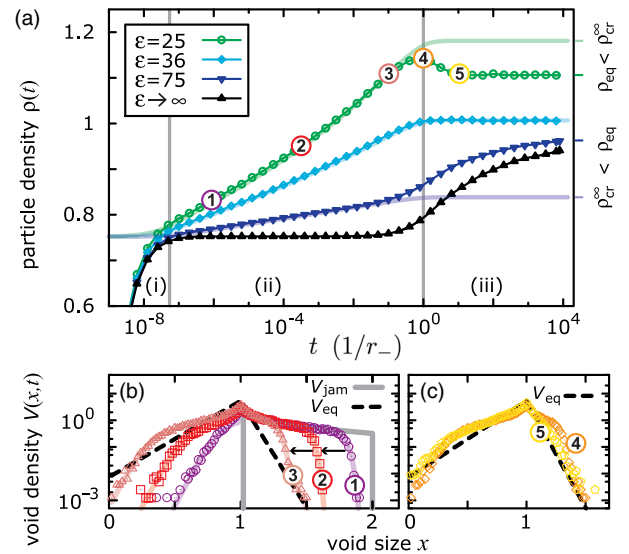


FIG. 2 (color online). Soft particle adsorption-desorption kinetics. (a) Density evolution for different stiffnesses ε with $\mu = 20$. Symbols: stochastic simulations; transparent overlays: crammering dynamics of Eq. (6). Vertical lines indicate the adsorption and desorption time scales. (b), (c) Gap size distribution for $\varepsilon = 25$ at the time points marked in (a). At the onset of crammering, $V(x, t)$ is similar to the jammed distribution $V_{\text{jam}}(x)$.

density of hard-core particles approaches ρ_{eq} extremely slowly from below, soft particles can either reach ρ_{eq} from below, arrive directly at ρ_{eq} at the onset of the third stage, or display a density overshoot before rapidly relaxing to ρ_{eq} from above.

The surprisingly rich kinetic behavior of Fig. 2(a) calls for a clarification of the underlying physics. How does the logarithmic behavior in stage (ii) arise from the softness and how generic is it? Under which conditions does nonmonotonic filling occur in an adsorption-desorption process that obeys detailed balance? Why is the relaxation to thermodynamic equilibrium much faster for soft particles? We address these questions in the remainder of this article by combining numerical analysis with analytical arguments.

Cramming.—The physics underlying the logarithmic regime (ii) of Fig. 2(a) is revealed by Fig. 2(b), which shows three consecutive snapshots of the void distribution $V(x, t)$. At the onset of stage (ii), $V(x, t)$ is similar to the known jammed distribution $V_{\text{jammed}}(x)$ for irreversibly adsorbed hard particles [24],

$$V_{\text{jammed}}(x) = 2 \int_0^\infty dt t \exp \left[-(x-1)t - 2 \int_0^t du \frac{1-e^{-u}}{u} \right] \quad (5)$$

[for $1 \leq x < 2$, while $V_{\text{jammed}}(x) = 0$ otherwise]: Both distributions display a dropoff for large gaps, while voids $x < 1$ are suppressed in $V(x, t)$ and are entirely forbidden in $V_{\text{jammed}}(x)$. With increasing time, the dropoff in $V(x, t)$ progressively moves to smaller x as the largest available voids are filled (creating new voids with $x < 1$). This behavior indicates that the system's memory of the jammed configuration generated in stage (i) governs the ‘‘cramming’’ dynamics during stage (ii).

We quantify this physical picture by considering the Langmuir kinetics of reversibly filling the gaps in a jammed configuration. If $P(x, t)$ denotes the probability that a void of size x remains unfilled at time t , we have $P(x, t) = [\gamma_+(x)e^{-(\gamma_+(x)+r_-)t} + r_-]/[\gamma_+(x) + r_-]$, where $\gamma_+(x) = \int_0^x dy \tilde{r}_+(y, x-y)$ is an effective filling rate that combines all attachment possibilities. Neglecting multiple filling, this yields the cramming dynamics

$$V_{\text{cr}}(x, t) = P(x, t)V_{\text{jammed}}(x) + 2 \int_x^\infty dx' [1 - P(x', t)] \times V_{\text{jammed}}(x') \frac{\tilde{r}_+(x, x'-x)}{\gamma_+(x')}, \quad (6)$$

which can be considered an approximate solution to Eq. (4) for the cramming stage [20]. This distribution and the corresponding density $\rho_{\text{cr}}(t) = \int_0^\infty dx V_{\text{cr}}(x, t)$ are displayed as semitransparent lines in Fig. 2, showing that Eq. (6) captures the kinetics of stage (ii) very well. It also

explains the logarithmic increase of $\rho(t)$: Approximating $\gamma_+(x)$ by its largest contribution, the drop in $V(x, t)$ moves as $\Delta x_{\text{dr}}(t) := 2 - x_{\text{dr}}(t) \approx \ln(r_+ t)/\varepsilon$ for our linear potential [20]. Given that the density is related to the area under the void size distribution, this yields [20]

$$\Delta \rho(t) \approx V_{\text{jammed}}(2) \ln(r_+ t)/\varepsilon, \quad (7)$$

which rationalizes the logarithmic time dependence and predicts how the dynamics slow down with increasing stiffness ε .

Nonmonotonic density.—Remarkably, $\rho(t)$ can transiently exceed the equilibrium density. We now show that this is a result of desorption erasing the memory of stage (i) that was preserved during stage (ii). We first note that the density $\rho_{\text{cr}}(t)$ obtained above (by assuming that only cramming is reversible while the underlying jammed configuration is preserved) saturates towards a value ρ_{cr}^∞ , which can be smaller than the equilibrium density ρ_{eq} [the blue line in Fig. 2(a)], or can exceed it (the green line). Figure 3(a) shows that the parameter regime where $\rho_{\text{cr}}^\infty > \rho_{\text{eq}}$ is virtually identical with the regime where the maximal density ρ_{max} exceeds ρ_{eq} . Thus, a nonmonotonic density $\rho(t)$ occurs whenever suppressing rearrangements leads to a larger equilibrium density than allowing for them.

To elucidate the minimal requirements for nonmonotonic filling and to study the phenomenon from the perspective of nonequilibrium thermodynamics, it is useful to consider the case of dimers on a discrete lattice. For soft dimers, which can overlap by a single site at the energetic cost $\varepsilon/2$, nonmonotonic filling occurs in a similar parameter range as in the continuum model; see Fig. 3(b). In fact, the boundaries in (ε, μ) space can be understood with a simple argument: A density overshoot is possible only if single overlaps occur faster than desorption and simultaneous overlaps with both neighboring particles are rare, which translates into the condition [20]

$$\varepsilon/2 < \mu < \varepsilon. \quad (8)$$

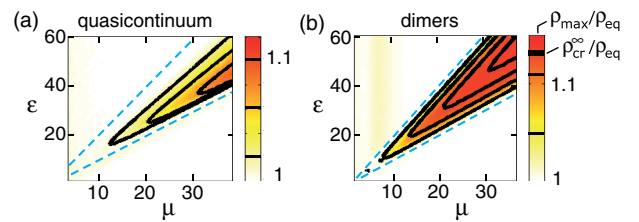


FIG. 3 (color online). Phase diagram in (ε, μ) space for the density overshoot with (a) quasicontinuum particles and (b) soft dimers. The overshoot is the ratio of the maximum and the equilibrium densities $\rho_{\text{max}}/\rho_{\text{eq}}$ observed numerically (color coded). Overlaid are contour lines of $\rho_{\text{cr}}^\infty/\rho_{\text{eq}}$, where ρ_{cr}^∞ is the asymptotic cramming density derived from Eq. (6). Dashed lines indicate the regime of Eq. (8).

This regime is indicated by the dashed lines in Fig. 3. Interestingly, this regime also encompasses the nonmonotonic region of the continuum model, showing that Eq. (8) provides a necessary (but not sufficient) condition for the class of models that we consider.

Why can a density overshoot occur for soft but not for hard particles? One way to address this question is to consider the large- ε behavior of the lattice equivalent of Eq. (4). After the initial filling stage, the only relevant components of the void density vector for soft dimers are the ones for overlapping dimers, for adjacent dimers, and for single empty sites. Space conservation then reduces the dynamics to a two-dimensional first-order ordinary differential equation, which permits nonmonotonic behavior (see the Supplemental Material [20] for details). However, in the limit $\varepsilon \rightarrow \infty$, the dynamics become effectively one dimensional, and hence monotonic, since the overlapping dimer degree of freedom is lost. Thus, the mathematical mechanism within the mean field description is dimensional reduction.

Nonequilibrium thermodynamics.—Figure 4 shows the filling dynamics $\rho(t)$ of dimers together with two thermodynamic quantities, S and H . The time-dependent entropy $S(t) = -(1/L)\sum_n p_n(t) \log p_n(t)$ can be computed via the occupation probabilities $p_n(t)$ of all configurations of the system (we measure the system size L in units of the particle size). It displays a nonmonotonic behavior, not only for soft dimers (the dashed line) but also for hard dimers (the solid line), which is not surprising since our system is initially far from equilibrium. That $S(t)$ first rises and later decreases during relaxation is consistent with the

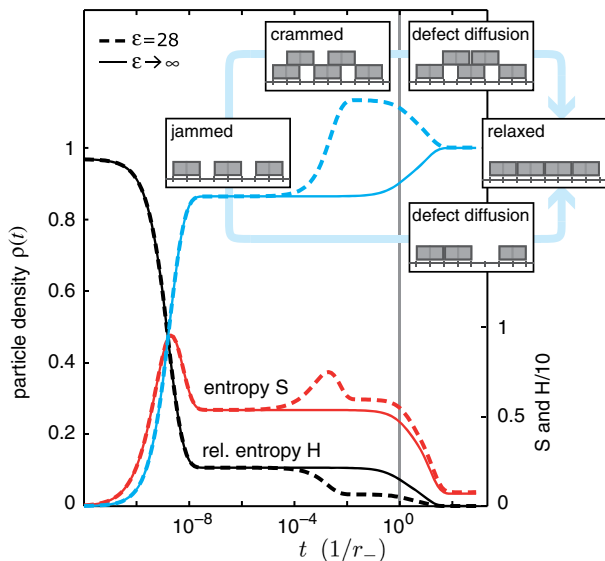


FIG. 4 (color online). Evolution of the density (left axis) and thermodynamic quantities (right axis) for hard (solid) and soft (dashed) dimers ($\mu = 20$). Soft dimers may overlap by one site at the cost of the interaction energy $\varepsilon/2 = 14$. Relevant stages for hard (bottom path) and soft (top path) dimers are sketched.

evolution from a single initial state (empty) through disordered intermediate states to a highly ordered equilibrium state (relevant stages are sketched in Fig. 4). However, the relative entropy $H(t) = (1/L)\sum_n p_n(t) \log[p_n(t)/p_n^{\text{eq}}]$ (with respect to the equilibrium state) must monotonically decrease for a system described by a discrete master equation that obeys detailed balance [25]. Figure 4 shows that the density overshoot is compatible with this fundamental theorem.

Relaxation kinetics.—Figure 2 indicated that relaxation to equilibrium is faster for soft particles than for hard. To clarify whether the relaxation behavior is qualitatively different, we examine how $|\rho(t) - \rho_{\text{eq}}|$ approaches zero in Fig. 5 (and in more detail in the Supplemental Material [20]). For dimers, the relaxation behavior is actually the same for hard and soft particles, due to a particle-hole symmetry [20]: Both jamming (for hard particles) and cramming (for soft particles) lead to configurations with “defects,” which undergo a diffusion-annihilation process. For hard particles, the defects are isolated, unoccupied lattice sites, and diffusion occurs via desorption of an adjacent particle followed by immediate adsorption of a particle into the gap [22]. The progressive dilution of defects leads to the power law behavior $|\rho(t) - \rho_{\text{eq}}| \sim t^{-1/2}$, which holds until the finite defect creation rate balances the diffusion-annihilation process. For soft particles, the defects are sites with double occupancy, which by a similar mechanism lead to the same power law behavior and even a “mirror symmetry” of the relaxation curve around density one [20].

This symmetry is broken when the particle size is increased to k -mers with $k > 2$ (since reactions then occur between defects of different sizes). Figure 5 shows that for hard particles the relaxation behavior becomes *slower* as k increases, while it becomes *faster* for soft particles. The scaling approaches logarithmic behavior in the limit $k \rightarrow \infty$ for hard particles [11,12], while it approaches exponential behavior for soft particles. Qualitatively, this is explained by the fact that the soft interaction “guides” attaching particles to the most favorable positions (reducing the entropic barrier for the rearrangements required for equilibration). Other shapes of the interaction potential lead

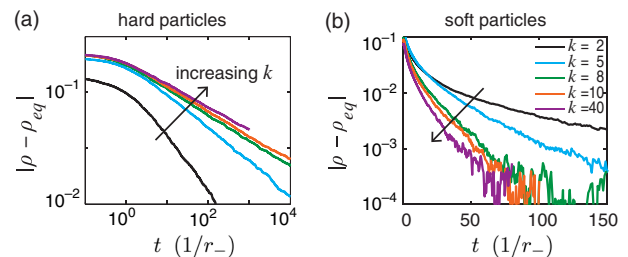


FIG. 5 (color online). Equilibration behavior of hard (a) and soft (b) particles with different sizes k on a lattice ($\mu = 30$). For hard particles, the relaxation kinetics slows with increasing k , while it becomes faster for soft particles ($\varepsilon = 36$).

to the same behavior as long as the repulsion is sufficiently soft [20].

Discussion.—We have shown that the adsorption-desorption kinetics of soft particles differs fundamentally from that of hard particles in at least three aspects: (i) the jamming behavior, with a gradual density increase instead of the Rényi plateau, (ii) a density overshoot, which can occur only for soft particles, on a time scale set by the desorption rate, and (iii) the relaxation behavior, which for soft particles becomes faster with increasing particle size (on a lattice), while hard particles show the opposite trend. We performed our analysis for a minimal model and showed that our qualitative conclusions are not sensitive to details such as the precise shape of the repulsive interaction potential and the way in which it affects the kinetic rates.

Models within this class are directly relevant in biophysics, for instance, in describing the binding of dimeric kinesins to microtubules [26] (where the softness stems from the ability to bind with either one or two head domains) or the assembly of nucleosome arrays [15] (where the softness arises from transient, thermally induced DNA unwrapping). While our analysis was limited to 1D substrates, we expect that much of the qualitative phenomenology carries over to 2D substrates. An interesting 2D experimental system is protein adsorption from blood plasma, which can show nonmonotonic surface density [27–29]. This effect is not well understood but is usually interpreted in a two-species scenario where a fast-binding protein is replaced by a slower but stronger-binding competitor. Our findings suggest that even a single soft protein species could generate nonmonotonic densities.

Another field of application is the physics of vibrated granular materials. The sluggish kinetics of these systems is nonadiabatic and shows signs of broken ergodicity [30,31]. One-dimensional models have already been useful to describe certain aspects of these kinetics phenomenologically [13,32]. The introduction of an effective soft-core interaction will provide a valuable new dimension in the parameter space of such phenomenological descriptions. More generally, it will be interesting to explore how the rich adsorption-desorption kinetics of soft particles couples to other kinetic processes. For instance, it should modify the collective dynamics of molecular motors, reaction-diffusion processes that involve a lower-dimensional substrate, and substrate-guided self-assembly processes.

*gerland@tum.de

- [1] W. Evans, *Rev. Mod. Phys.* **65**, 1281 (1993).
 [2] J. D. McGhee and P. H. von Hippel, *J. Mol. Biol.* **86**, 469 (1974).
 [3] J. Krug and T. Michely, *Islands, Mounds and Atoms*, Springer Series in Surface Sciences (Springer, New York, 2004).

- [4] J. Feder, *J. Theor. Biol.* **87**, 237 (1980).
 [5] J. Talbot, G. Tarjus, P. R. Van Tassel, and P. Viot, *Colloids Surf., A* **165**, 287 (2000).
 [6] J. Flory, *J. Am. Chem. Soc.* **61**, 1518 (1939).
 [7] J. Toner and G. Y. Onoda, *Phys. Rev. Lett.* **69**, 1481 (1992).
 [8] R. Padinhateeri and J. F. Marko, *Proc. Natl. Acad. Sci. U.S.A.* **108**, 7799 (2011).
 [9] A. Rényi, *Publ. Math. Inst. Hung. Acad. Sci.* **3**, 109 (1958); Selected translations in mathematical statistics and probability **4**, 203 (1963).
 [10] S. F. Edwards and R. B. S. Oakeshott, *Physica (Amsterdam)* **157A**, 1080 (1989).
 [11] X. Jin, G. Tarjus, and J. Talbot, *J. Phys. A* **27**, L195 (1994).
 [12] P. L. Krapivsky and E. Ben-Naim, *J. Chem. Phys.* **100**, 6778 (1994).
 [13] E. Ben-Naim, J. B. Knight, E. R. Nowak, H. M. Jaeger, and S. R. Nagel, *Physica (Amsterdam)* **123D**, 380 (1998).
 [14] J. Mattsson, H. M. Wyss, A. Fernandez-Nieves, K. Miyazaki, Z. Hu, D. R. Reichman, and D. A. Weitz, *Nature (London)* **462**, 83 (2009).
 [15] B. Osberg, J. Nuebler, P. Korber, and U. Gerland, *Nucleic Acids Res.* **42**, 13633 (2014).
 [16] M. van Hecke, *J. Phys. Condens. Matter* **22**, 033101 (2010).
 [17] J. B. Knight, C. G. Fandrich, C. N. Lau, H. M. Jaeger, and S. R. Nagel, *Phys. Rev. E* **51**, 3957 (1995).
 [18] J. Talbot, G. Tarjus, and P. Viot, *Phys. Rev. E* **61**, 5429 (2000).
 [19] P. Richard, M. Nicodemi, R. Delannay, P. Ribière, and D. Bideau, *Nat. Mater.* **4**, 121 (2005).
 [20] See Supplemental Material at <http://link.aps.org/supplemental/10.1103/PhysRevLett.115.088301>, which includes Ref. [21], for elaborated presentations of several arguments and numerical methods.
 [21] W. Möbius, B. Osberg, A. M. Tsankov, O. J. Rando, and U. Gerland, *Proc. Natl. Acad. Sci. U.S.A.* **110**, 5719 (2013).
 [22] P. L. Krapivsky, S. Redner, and E. Ben-Naim, *A Kinetic View of Statistical Physics* (Cambridge University Press, Cambridge, England, 2010).
 [23] D. T. Gillespie, *J. Phys. Chem.* **81**, 2340 (1977).
 [24] G. Tarjus and P. Viot, *Phys. Rev. E* **69**, 011307 (2004).
 [25] N. G. van Kampen, *Stochastic Processes in Physics and Chemistry*, Third ed. (Elsevier, New York, 2007).
 [26] E. Frey and A. Vilfan, *Chem. Phys.* **284**, 287 (2002).
 [27] S. L. Hirsh, D. R. McKenzie, N. J. Nosworthy, J. A. Denman, O. U. Sezerman, and M. M. M. Bilek, *Colloids Surf., B* **103**, 395 (2013).
 [28] L. Vroman, A. L. Adams, G. C. Fischer, and P. C. Munoz, *Blood* **55**, 156 (1980).
 [29] J. L. Brash and P. ten Hove, *Thromb. Haemostas.* **51**, 326 (1984).
 [30] A. J. Kolan, E. R. Nowak, and A. V. Tkachenko, *Phys. Rev. E* **59**, 3094 (1999).
 [31] F. Paillusson and D. Frenkel, *Phys. Rev. Lett.* **109**, 208001 (2012).
 [32] E. R. Nowak, J. B. Knight, E. Ben-Naim, H. M. Jaeger, and S. R. Nagel, *Phys. Rev. E* **57**, 1971 (1998).